Supporting Information

Title: **Unveiling the crystallographic effect of $Li(Ni_{0.90}Co_{0.09}Al_{0.01})O_2$ with a high Ni content on the high capacity generation in Li-ion battery**

Junghwan Park[1,] and Pilgyu Byeon[1]*

[1]Analysis Group, R&D center, Samsung SDI, 130, Samsung-ro, Yeongtong-gu, Suwon-si, Gyeonggi-do, Korea

*Corresponding author: hwan2k.park@samsung.com

Keywords: A high Ni cathode material, A high capacity, Anisotropic strain, In-situ XRD, Crystallographic properties, Li-ion battery

We confirmed the morphology and crystallography of $Li(Ni_{0.90}Co_{0.09}Al_{0.01})O_2$ powder before making a cathode electrode in a Li-ion cell. Fig. 1S(a) shows the morphology properties of $Li(Ni_{0.90}Co_{0.09}Al_{0.01})O_2$ particles obtained with SEM measurement. The diameter of a particle is about 16 μm as shown in the surface morphology. The cross-section of a particle with a magnitude of 50,000 times verifies the similarity between the interior and the surface of a particle. The SEM results prove that the grain homogenously grew up about 1 μm both inside and outside the particle. Fig. 1S(b) shows the internal structure of the particle that was observed by TEM measurement. The result of ADF-STEM displays bright points that indicate individual electron scattering events at the center in Fig. 1S(b). It is the main effect of transition metals (Ni, Co, and Al) because the scattering effect of Li and O is weak. TM atoms in $Li(Ni_{0.90}Co_{0.09}Al_{0.01})O_2$ are well arranged in layers along the c-axis of the hexagonal structure. The left in Fig. 1S(b) is the FFT pattern that was obtained from the ADF-TEM image. The diffraction pattern is indexed with the hexagonal structure of *R-3 m* corresponding to the zone axis of [010]. Fig. 1S(c) is the result of Raman spectroscopy of the crystal structure for the surface of powders. Our data was fitted as the best with two peaks which are respectively observed at 580 and 497 cm^{-1}. The identification of crystal structure is established with the phonon Raman active modes of A_{1g} and E_g. The A_{1g} mode is the

symmetrical stretching of TM–O for atomic displacement parallel to the c-axis whereas the E_g mode is the symmetrical deformation for atomic displacement perpendicular to the c-axis. The powder XRD measurement was carried out at room temperature to verify the global crystal structure of $Li(Ni_{0.90}Co_{0.09}Al_{0.01})O_2$. Fig. 1S(d) is the result of refinement for XRD data by the Rietveld method with the model of the layered hexagonal structure of *R -3 m*. The circles are the data and the lines are the best fits. The bars under the data indicate the positions of the calculated Bragg peaks. The difference between the data and fit is shown at the bottom of the figure. We achieved good agreement factors of $\chi^2 = 3.2$, $R_p = 1.7$ %, and R_{wp}=2.5 %. Lattice parameters are a= 2.87287(1) Å and c= 14.19231(1) Å. The volume of the unit cell is V= 101.441(1) $Å^3$. Atomic positions and occupancy in the unit cell were obtained as shown in Table 1 and all atoms are uniformly distributed by the desired amount. The result of complementary measurements proves the exact layered hexagonal structure for the global and local range of our sample. And we graphically obtained Fig. 1S(e) that these atoms form the two octahedral structures of Li-O_6 and TM-O_6.

Fig. 1S. (a) SEM images show the morphology properties of a surface (the right and the left figure) and a cross-section (center) for the particle of $Li(Ni_{0.90}Co_{0.09}Al_{0.01})O_2$. (b) TEM results of STEM-ADF (center) and FFT pattern (left) confirm the internal structure of a material with the hexagonal structure of *R -3 m*. (c) Raman spectrum shows two vibrational components of the hexagonal structure. It is divided into two peaks of E_g of 497 cm^{-1} and A_{1g} of 580 cm^{-1}. (d) The refinement result of XRD data is obtained with using space group *R -3 m*. The black circles and red lines are the experimental data and best fit. The bottom of the figure shows the difference between the data and fit. The calculated Bragg peaks with the hexagonal structure model are indicated with the bars under the data. (e) The hexagonal structure of $Li(Ni_{0.90}Co_{0.09}Al_{0.01})O_2$ is presented as the figure from various experimental measurements.

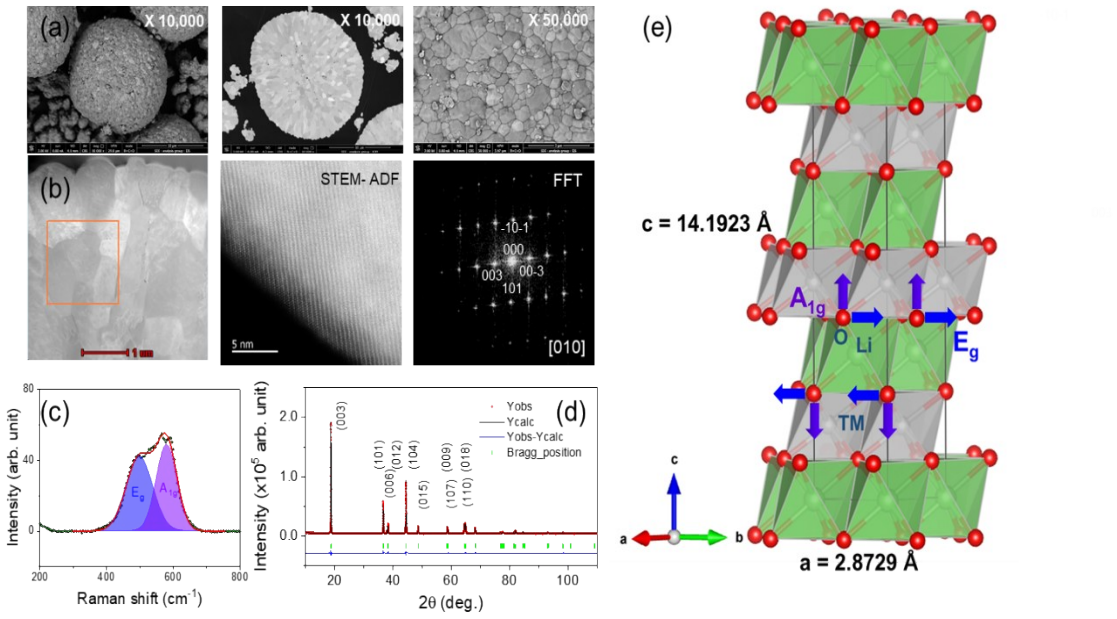

Fig. 2S. The results of *in-situ* XRD measurement are shown for (a) 2 cycles with 0.1C, (b) 2 cycles with 0.5C, and (c) 5 cycles with 1C.

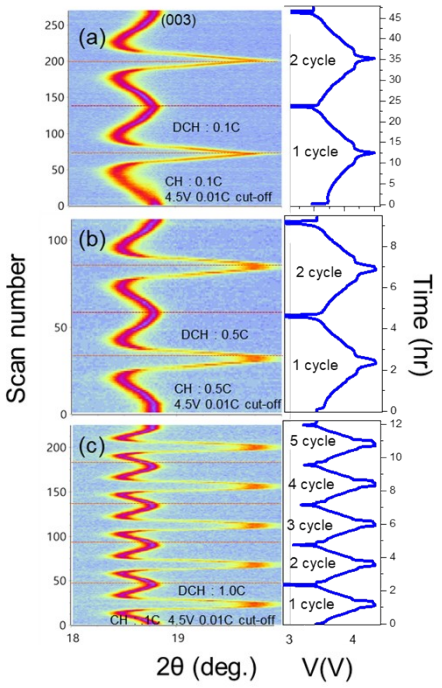

Fig. 3S. The *in-situ* XRD is measured at two scattering angle ranges at (a) 25, (b) 35, and (c) 45 ℃ to obtain the lattice constant a and c from two peaks of (003) and (101).

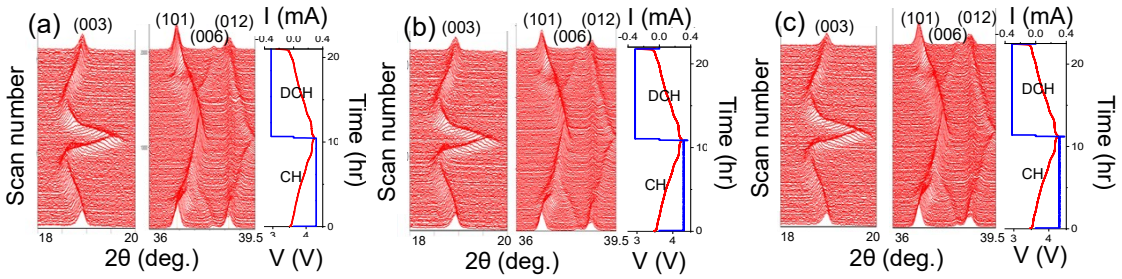

Fig. 4S. (a) The refinement results for XRD data of SOC 0, 50, and 100% are obtained with using space group R -3 m. The black circles and the red line are the experimental data and best fit. The bottom of the figure shows the difference between the data and fit. The calculated Bragg peaks with the hexagonal structure model are indicated with the bars under the data.

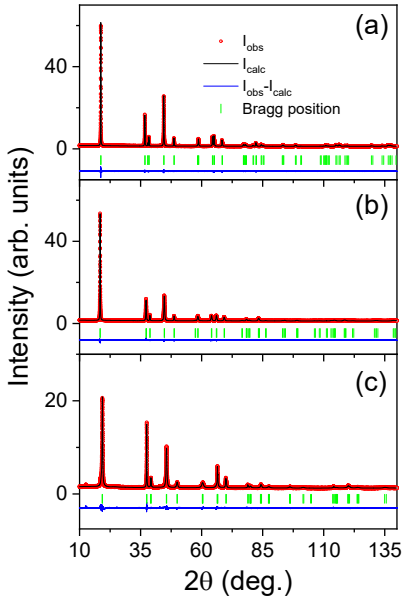

Table 1S. XRD data of $Li(Ni_{0.90}Co_{0.09}Al_{0.01})O_2$ is refined with the Rietveld method to obtain the crystallographic information that is lattice constants, the unit-cell volume, atom position, and atom occupancy.

Crystal structure		**$Li(Ni_{0.90}Co_{0.09}Al_{0.01})O_2$**
Lattice constant (Å)	a	2.87287 (1)
	c	14.19231 (6)

Volume (Å^3)	V	101.441 (1)
Oxygen position	Oz	0.24131 (6)
Occupancy	3a Li	1.00(1)
	3b Ni	0.90(1)
	3b Co	0.09(1)
	3b Al	0.01(1)
Agreement factors	R_p (%)	2.24
	R_{wp} (%)	3.18
	χ^2	1.30